Hybridization of angular-momentum eigenstates in nonspherical sodium clusters

C. Bartels,[1] C. Hock,[2] R. Kuhnen,[2] M. Walter,[2] and B. v. Issendorff[2]
[1]*Institut für Physikalische Chemie, Universität Göttingen, 37077 Göttingen, Germany*
[2]*Fakultät für Physik, Universität Freiburg, 79104 Freiburg, Germany*
(Received 28 October 2011; published 17 October 2013)

Angle-resolved photoelectron spectra of low-temperature sodium clusters Na_{33}^- and Na_{34}^- have been measured as a function of photon energy. The experiments in combination with density functional theory calculations demonstrate that despite the strongly oblate shape of the clusters, most of the occupied valence orbitals are close to angular-momentum eigenstates. Some states, however, exhibit a strongly mixed character. This mixing follows the selection rules $\Delta l = \pm 2$ and $\Delta m = 0$, which result from the approximate symmetry of the cluster deformation.

DOI: 10.1103/PhysRevA.88.043202 PACS number(s): 36.40.Cg, 33.60.+q, 73.22.−f

I. INTRODUCTION

Quantum dots and nanoparticles are often referred to as artificial atoms [1] or superatoms [2,3] because in these systems delocalized states exist that resemble the angular-momentum eigenstates of an isolated atom. In simple metal particles, the characteristic degeneracy of these states leads to the well-known electron shell structure [4–9], the influences of which have been found in many of their properties [7]. The general size dependence of these properties can be explained by simple spherical free-electron-gas models [5]; even better agreement with the experimental data can be achieved if the influence of nonspherical shapes is taken into account, employing, e.g., modified Nilsson models [10] or density functional theory (DFT) calculations in the spheroidal [11] or ellipsoidal jellium approximation [12,13].

Nevertheless, the question remains to which detail such free-electron models can describe the electronic structure of a metal cluster. A real cluster never has perfect spherical (or cylindrical) symmetry because of its internal atomic structure and its correspondingly nonspherical outer shape. Consequently, the angular momentum of the electrons or its projection cannot be good quantum numbers; the true electronic single-particle eigenstates are always superpositions of an infinite number of different angular-momentum eigenstates. Therefore, the question of how good the superatom picture is could be reformulated as the question of how strongly different angular-momentum eigenstates are mixed. This mixing will get stronger with increasing electron-ion interaction, with the deviation from sphericity, as well as with cluster size [14]. In the case of aluminum, for example, the rather strong interaction of the electrons with the triply charged background ions as well as the often strongly faceted cluster surface cause significant deviations from the spherical jellium model predictions [15]. But even in the case of sodium, which is considered to be the closest representative of a free-electron metal [16], the perturbing influences of the internal ionic structure and the cluster surface lift the degeneracy of the angular-momentum eigenstates and broaden these shells into bands of a width comparable to the average energetic shell-shell distances [17,18]. With the help of angle-resolved photoelectron spectroscopy, we recently showed that in close to spherical sodium clusters the valence orbitals still resemble angular-momentum eigenstates [18], despite the presence of these perturbing effects. We have now applied the same technique to probe the valence-electron orbitals of strongly nonspherical clusters, in which the combined influences of the discrete ionic background and the nonspherical overall shape could lead to a much stronger mixing of the electron shell states, and therefore potentially even to a breakdown of the superatom description.

For the measurements, we chose the clusters Na_{33}^- and Na_{34}^- because of their particular properties. In a spherical jellium model, Na_{33}^- would have the closed-shell electronic configuration $1s^2 1p^6 1d^{10} 2s^2 1f^{14}$, while Na_{34}^- would have an additional electron in a $2p$ orbital. Nevertheless, already simple models predict that Na_{33}^- does not adopt the spherical shape usually expected for electronically closed shell clusters, but instead exhibits a strong oblate deformation [10,13], due to hybridization between occupied $1f$ and unoccupied $2p$ levels [19]. It has been confirmed both by full atomistic calculations as well as experiments that the real cluster perfectly follows this prediction: Na_{33}^- adopts a strongly oblate and well-packed C_{5v} structure [17,20]. Na_{34}^- adopts the same structure with just the one missing vertex atom added, producing a highly symmetric (and still strongly oblate) D_{5h} structure [17,20]. This is in fact an example of a deviation from simple free-electron-model behavior, as most models predict a prolate deformation for a 35-electron cluster [10,13].

II. EXPERIMENTAL METHODS

In the experiments, the same setup was used as for the study on spherical sodium clusters [18]. Briefly, the clusters were produced by evaporating sodium into a liquid-nitrogen-cooled helium atmosphere of approximately 1 mbar pressure, and charged by a pulsed electric discharge. They were then stored in a radiofrequency ion trap, which was cooled to 6 K by a closed-cycle helium refrigerator, and thermalized by collisions with helium buffer gas. After pulsed extraction from the trap and mass selection in a time-of flight mass spectrometer, the clusters were irradiated with linearly polarized light from a nanosecond dye laser. The resulting photoelectrons were detected in a velocity-map-imaging spectrometer [21,22]. Their original three-dimensional distributions were reconstructed from the measured projections by a slightly modified version

of the pbasex algorithm [23], and the average anisotropies for electrons detached from a given level were determined by least-squares fits to these reconstructions [24]. For single-photon absorption and linear polarization, the photoelectron angular distribution is restricted to the form $1 + \beta P_2(\cos\theta)$, where P_2 is the second Legendre polynomial, θ is the electron emission angle with respect to the laser polarization, and β is the anisotropy parameter [25], which is related to the angular momentum of the bound state of the electron [26,27]. Angle-resolved spectra have been measured for 28 photon energies between about 1.6 and 4 eV.

III. THEORETICAL METHODS

For the calculations, a real-space-grid projector-augmented-wave method [28] was used, where the exchange correlation energy was approximated by taking gradient corrections into account [29]. Spin polarization was considered for the energetics of systems with unpaired spins. The cluster structures taken from Ref. [17] were rerelaxed but stayed practically unchanged. To avoid the spurious spin splitting of the photoelectron peaks [30], the densities of states of spin-paired calculations were used for the evaluation of the photoelectron spectra.

IV. EXPERIMENTAL RESULTS

Figure 1 shows photoelectron spectra of the two clusters, measured at a wavelength of 462 nm (a photon energy of 2.68 eV). The respective lower panels show the angle-resolved spectra, the upper panels the angle-integrated ones. The distinct peaks in the spectra are associated with electron detachment from different orbitals. To facilitate the discussion, the peaks are labeled by letters A to F for Na_{33}^-, and by A' to F' for Na_{34}^-. Peak C' of Na_{34}^- in fact is at least a double peak, but it has been assigned a single letter as for higher photon energies the splitting could not be resolved anymore (meaning that the energy dependence of the angular distributions could not be evaluated for the two peaks separately). As has been shown earlier [17], in the case of Na_{34}^- the uppermost peak (A') is clearly separated from the rest of the spectrum, which indicates that here one electron is added to a closed shell system, exactly as one would expect for the simple spherical jellium electronic configuration mentioned above. The angle-resolved spectra, however, give direct evidence that the situation is more complex, which is probably due to the nonspherical shape of the clusters. Earlier experiments have shown that in the case of close to spherical clusters, electrons emitted from states with the same approximate angular momentum and with similar kinetic energies exhibit very similar angular distributions [18]. We can tentatively assign electron shell quantum numbers to the different states in the spectra in Fig. 1 based on the general shell filling patterns visible in the size dependence of the photoelectron spectra of sodium clusters [17]. For example, the peaks A–D for Na_{33}^- and B'–D' for Na_{34}^- should be $1f$ states, while the uppermost A' should be a $2p$ state. This assignment should be reflected in the angular distributions of the photoelectrons, which clearly is not the case. At this photon energy, peaks A and C of Na_{33}^- exhibit parallel distributions (electron emission dominantly into the direction of the laser

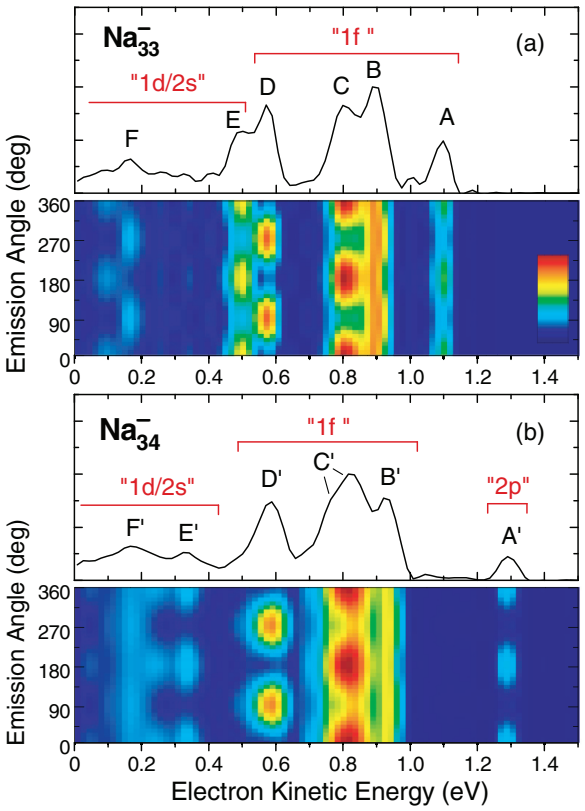

FIG. 1. (Color online) (a) Angle-integrated and angle-resolved photoelectron spectra of Na_{33}^-, recorded at a photon energy of 2.68 eV. The electron emission angle is measured with respect to the laser polarization axis. (b) Spectra of Na_{34}^-, recorded at the same photon energy. The angular momentum assignment of the electronic states as expected for vanishing state mixing is indicated.

polarization), whereas B and D show perpendicular ones. For Na_{34}^-, A' exhibits a parallel distribution like peak C', while the distribution of B' is practically isotropic, and that of D' perpendicular. The different characters of the states can be seen even better in the photon-energy dependence of the angular distributions. We recorded angle-resolved photoelectron spectra at wavelengths ranging from 308 to 760 nm (photon energies from 1.63 to 4.02 eV). The angular distribution of a given peak in the spectrum can be quantified by the anisotropy parameter β, which takes values between -1 and 2 (see above). The energy dependence of the β parameter is strongly influenced by the character of the initial wave function of the emitted electron; it therefore can be used to identify states with similar (or dissimilar) wave functions [18]. In Fig. 2, the extracted β parameters are displayed as a function of the photoelectron kinetic energy. There are indeed pronounced differences between the β curves of the "$1f$" states A–D of Na_{33}^-, and there is no clear distinction between these and the curves of the other states; the same applies to Na_{34}^-. This seems to indicate that the cluster deformation leads to a rather strong scrambling of the electron wave-function characters. Nevertheless, one can make the surprising observation that there are strong similarities between the β curves of certain states of the two cluster sizes, namely between B and B', D and D', E and E', F and F', as well as C and A' and A and C'. This shows that despite the perturbing effect of the

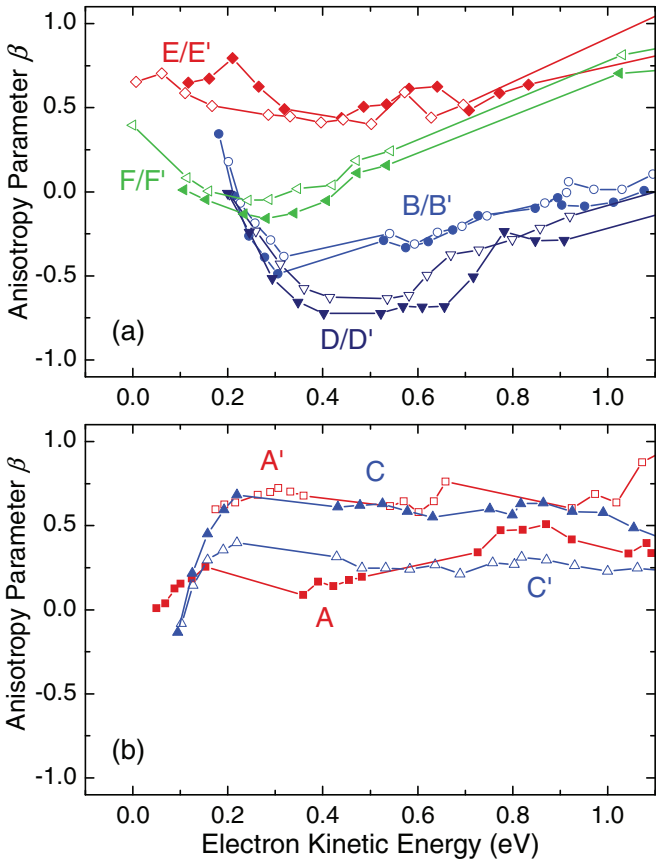

FIG. 2. (Color online) Photon energy dependence of the anisotropy parameters β. The values of β obtained from fits to the angular distributions of the different peaks labeled in Fig. 1 are plotted as a function of the resulting photoelectron kinetic energy (as described in [18]). (a) The cases in which states with corresponding labels exhibit similar behavior. (b) The cases in which states with different labels exhibit similar behavior.

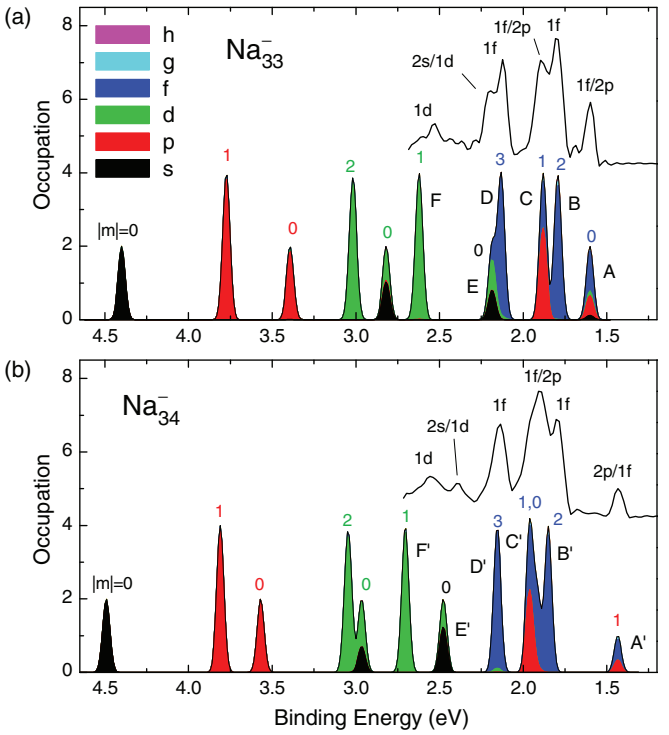

FIG. 3. (Color online) Calculated densities of states. The stick spectra of the Kohn-Sham energies were broadened by Gaussians with a width of 50 meV. The color coding and the numbers above the peaks indicate the contribution from different l, $|m|$ states, as obtained by an expansion of the Kohn-Sham orbitals in spherical harmonics. The experimental spectra recorded at 462 nm are shown for comparison. The peak lettering from Fig. 1 is used to indicate the assignment of the measured peaks. (a) Na_{33}^-. (b) Na_{34}^-.

nonspherical cluster structures, which leads to quite different overall densities of states of the two clusters and a complex pattern of the angular distributions, the characters of the wave functions of the different states are not at all arbitrary, but must follow a simple underlying rule.

V. COMPARISON TO THEORETICAL RESULTS

Density functional theory calculations demonstrate that this is indeed the case. The calculations were performed taking the full ionic structures into account, using the oblate ground-state geometries (a C_{5v} structure for Na_{33}^-, a D_{5h} one for Na_{34}^-) recently found in a combined experimental and theoretical study [17]. The angular-momentum decomposition of the Kohn-Sham orbitals was calculated by an expansion in spherical harmonics [31]. Figure 3 shows the results along with the experimental angle-integrated spectra. The agreement between the calculated densities of states and the measured photoelectron spectra is excellent, underlining the reliability of the calculations. Although, as mentioned before, in principle neither the angular momentum nor its projection onto a principal axis is a good quantum number in a real cluster due to its discrete atomic structure, the calculated orbitals are very close to what one would expect within a spheroidal jellium model. This is already suggested by the shape of the orbitals (images are shown in the Supplemental Material [32]) and is confirmed by the spherical harmonic expansion. The color coding in Fig. 3 reflects the relative contributions of the different angular momenta. One can see that all orbitals are either almost pure angular momentum eigenstates or mixed from two eigenfunctions that differ by $\Delta l = \pm 2$, with negligible contributions from other angular momenta. Because of the oblate shape of the clusters, the angular-momentum eigenstates are not $(2l + 1)$-fold degenerate, but split into $l + 1$ levels with different values of $|m|$ (the $\pm m$ degeneracy is approximately retained). The $|m|$ values are indicated above each peak; note that the energetic sequence of the states is close to that predicted by the simple Clemenger-Nilsson model [10]. Mixing occurs only between states with the same value of $|m|$. The reason is that the oblate deformation of the clusters can be described as a quadrupolar perturbation of a spherical potential of the form Y_{20} (a spherical harmonic with $l = 2$ and $m = 0$) [25]. In such a case, the perturbed eigenfunctions are formed from the unperturbed eigenfunctions $|lm\rangle$ by admixing other eigenfunctions $|l'm'\rangle$, the degree of mixing being zero unless $\Delta l = \pm 2$ and $\Delta m = 0$.

The association of the peaks in the experimental spectra with the theoretical states is straightforward and can be used to explain the different energy dependencies of the corresponding

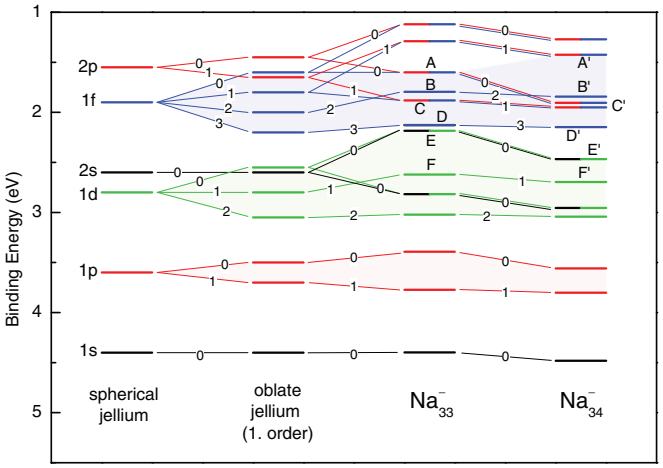

FIG. 4. (Color online) Energy-level correlation diagram. The calculated level structures of Na_{33}^- and Na_{33}^- are compared to the schematic level structures of a spherical and an oblate jellium cluster (the latter in first-order perturbation theory, i.e., with state mixing neglected). Lines connect states with the same l,$|m|$ character; the values of $|m|$ are given.

β values. The peaks F and F' can be both interpreted as $1d$, $|m| = 1$ states, which obviously is the reason why they exhibit very similar β curves. The peaks E and E', on the other hand, belong to $m = 0$ states, which are rather strong mixtures of $2s$ and $1d$. This explains the similarities of the β curves of E and E', as well as the difference between the pairs F and F' and E and E'. Accordingly, the close to identical behavior of the pairs D and D' and B and B' can be traced back to the fact that they are practically pure $1f$ states (with $|m| = 3$ and 2, respectively). Additionally, this shows that not only the angular momentum l, but also its projection $|m|$ determines the angular distributions, as there are small but significant differences between the curves of the two pairs. The most interesting cases are the states A and A' and C and C'. The peak A' of Na_{34}^- is associated with the singly occupied state above the "band gap" of neutral Na_{34}, which is a strongly mixed $1f/2p$ state with $|m| = 1$. Its β curve exhibits a strong similarity to that of peak C of Na_{33}^-, which is a mixed $1f/2p$ state with $|m| = 1$ as well. Peak A, on the other hand, is a $1f/2p$ state with $m = 0$, and accordingly behaves differently than peak A'. Its β curve does have some similarity to that of C', which indeed has a significant contribution from the $1f/2p$ state with $m = 0$. Nevertheless, peak C' also has a strong contribution of $1f/2p$, $|m| = 1$, which can explain the deviations between the β curves of A and C'.

In total, this shows that all of the electronic states visible in the photoelectron spectra have a well-defined (pure or mixed) angular momentum character, which is clearly reflected in the angular distributions of the photoelectrons. What remains to be discussed is the peculiar sequence of these l,m states. This can be elucidated with the help of Fig. 4. Here on the left the lowest levels of a spherical jellium model are shown. The second column schematically indicates the first-order perturbation of this structure by an oblate deformation, that is, without taking hybridization into account. The $|m|$ quantum numbers are indicated; for an oblate deformation, the binding energy increases with $|m|$. On the right the calculated level structures of Na_{33}^- and Na_{34}^- (as already shown in Fig. 3) are presented; lines connect states of the same approximate l and $|m|$ quantum numbers. Following the selection rule $\Delta l = \pm 2$ and $\Delta m = 0$, the $2s$ and the $1d$ ($m = 0$) states hybridize to form two new mixed states, one at lower and one at higher energy. The same happens to the $m = 0$ and the $|m| = 1$ states of the $2p$ and $1f$ manifold. This is the reason why the $|m| = 3$ and 2 states still appear in the same sequence as in the perturbed jellium model, while the $|m| = 1$ and $m = 0$ states are strongly shifted in energy and appear out of sequence. Note that the orbital correlations shown here, which are based on the calculated results, are in perfect agreement with the correlations that can be directly read off the experimental results in Fig. 2.

VI. CONCLUSION

These findings demonstrate a surprisingly clear superatom behavior of deformed sodium clusters. Similar effects can be expected to occur in any finite-size Fermi system of approximate cylindrical symmetry.

ACKNOWLEDGMENTS

This research was supported by the Deutsche Forschungsgemeinschaft. M.W. acknowledges computational resources from FZ-Jülich.

[1] R. C. Ashoori, Nature (London) **379**, 413 (1996).
[2] W. Ekardt, Z. Phys. B **103**, 305 (1997).
[3] J. U. Reveles, P. A. Clayborne, A. C. Reber, S. N. Khanna, K. Pradhan, P. Sen, and M. R. Pederson, Nat. Chem. **1**, 310 (2009).
[4] J. Martins, R. Car, and J. Buttet, Surf. Sci. **106**, 265 (1981).
[5] W. D. Knight, K. Clemenger, W. A. de Heer, W. A. Saunders, M. Y. Chou, and M. L. Cohen, Phys. Rev. Lett. **52**, 2141 (1984).
[6] W. Ekardt, Phys. Rev. B **29**, 1558 (1984).
[7] W. A. de Heer, Rev. Mod. Phys. **65**, 611 (1993).
[8] M. Brack, Rev. Mod. Phys. **65**, 677 (1993).
[9] B. v. Issendorff, in *Handbook of Nanophysics*, edited by K. Sattler (CRC, Boca Raton, FL, 2011), Vol. 2.
[10] K. Clemenger, Phys. Rev. B **32**, 1359 (1985).
[11] W. Ekardt and Z. Penzar, Phys. Rev. B **38**, 4273 (1988).
[12] G. Lauritsch, P.-G. Reinhard, J. Meyer, and M. Brack, Phys. Lett. A **160**, 179 (1991).
[13] C. Yannouleas and U. Landman, Phys. Rev. B **51**, 1902 (1995).
[14] U. Röthlisberger and W. Andreoni, J. Chem. Phys. **94**, 8129 (1991).
[15] L. Ma, B. von Issendorff, and A. Aguado, J. Chem. Phys. **132**, 104303 (2010).
[16] N. W. Ashcroft and N. D. Mermin, *Solid State Physics* (Saunders College, Philadelphia, 1976).

[17] B. Huber, M. Moseler, O. Kostko, and B. v. Issendorff, Phys. Rev. B **80**, 235425 (2009).
[18] C. Bartels, C. Hock, J. Huwer, R. Kuhnen, J. Schwöbel, and B. v. Issendorff, Science **323**, 1323 (2009).
[19] T. Hirschmann, M. Brack, and J. Meyer, Ann. Phys. (NY) **506**, 336 (1994).
[20] A. Aguado and O. Kostko, J. Chem. Phys. **134**, 164304 (2011).
[21] H. Helm, N. Bjerre, M. J. Dyer, D. L. Huestis, and M. Saeed, Phys. Rev. Lett. **70**, 3221 (1993).
[22] A. T. J. B. Eppink and D. H. Parker, Rev. Sci. Instrum. **68**, 3477 (1997).
[23] G. A. Garcia, L. Nahon, and I. Powis, Rev. Sci. Instrum. **75**, 4989 (2004).
[24] C. Bartels, Ph.D. thesis, University of Freiburg, 2008.
[25] C. N. Yang, Phys. Rev. **74**, 764 (1948).
[26] H. Bethe, in *Handbuch der Physik*, edited by H. Geiger and K. Scheel (Springer, Berlin, 1933), pp. 475–484.
[27] J. Cooper and R. N. Zare, J. Chem. Phys. **48**, 942 (1968).
[28] J. Enkovaara, C. Rostgaard, J. J. Mortensen, J. Chen, M. Dulak, L. Ferrighi, J. Gavnholt, C. Glinsvad, V. Haikola, H. A. Hansen *et al*., J. Phys.: Condens. Matter **22**, 253202 (2010).
[29] J. P. Perdew, K. Burke, and M. Ernzerhof, Phys. Rev. Lett. **77**, 3865 (1996).
[30] M. Walter and H. Häkkinen, New J. Phys. **10**, 043018 (2008).
[31] M. Walter, J. Akola, O. Lopez-Acevedo, P. D. Jadzinsky, G. Calero, C. J. Ackerson, R. L. Whetten, H. Grönbeck, and H. Häkkinen, Proc. Natl. Acad. Sci. (USA) **105**, 9157 (2008).
[32] See Supplemental Material at http://link.aps.org/supplemental/10.1103/PhysRevA.88.043202 for images of the orbitals.